Studies of $K_2^0 \to \pi^+\pi^-$ Decay and Interference*

V. L. Fitch, R. F. Roth,† J. Russ,‡ and W. Vernon§
Palmer Physical Laboratory, Princeton University, Princeton, New Jersey
(Received 8 August 1967)

We describe a detailed study of the *CP*-violating decay $K_2^0 \to \pi^+ + \pi^-$ in an experiment performed at the Brookhaven AGS. In a search for an energy dependence in the branching ratio, BR = rate$(K_2^0 \to \pi^+ + \pi^-)$/rate$(K_2^0 \to$ all charged modes), we find between 0.95 and 2.45 GeV that if BR $\propto E^n$ then $n = 0.03 \pm 0.33$. Assuming $n = 0$, then BR $= (1.97 \pm 0.16) \times 10^{-3}$, yielding $|\eta_{+-}| = (1.91 \pm 0.09) \times 10^{-3}$. In an interference experiment at a mean momentum of 1.55 GeV/c, we observe $\cos\alpha = 1.00 \pm 0.21$, where α is the phase angle between the $K_2^0 \to \pi^+ + \pi^-$ decay amplitude and the $\pi^+\pi^-$ amplitude from coherent regeneration in uniformly distributed Be. A search for neutral currents yields a limit on the branching ratio of $K_2^0 \to \mu^\pm + \mu^\mp$ of 3.5×10^{-5} and $K_2^0 \to \mu^\pm + e^\mp$ of 8×10^{-6} (both 90% confidence levels). We measure the mass of the K_1^0 to be 497.44 ± 0.50 MeV.

I. INTRODUCTION

THE experiments described here are designed to elucidate the nature of the decay process $K_2^0 \to \pi^+ + \pi^-$.[1] In particular the experiments are concerned with (a) a more accurate determination of the branching ratio; (b) a search for an energy dependence in this branching ratio; (c) a measurement of the interference between the amplitude for decay to $\pi^+\pi^-$ and that resulting from coherent regeneration; and (d) as a by-product of these investigations a limit for the decay $K_2^0 \to \mu^+ + \mu^-$. Preliminary results from these experiments have already been presented.[2–4]

The experiments are discussed and analyzed within the framework of the following considerations. In the absence of external fields and material the time development of the K^0-$\bar{K}^0$ system is given by[5]

$$-d\psi/dt = (\Gamma + iM)\psi, \tag{1}$$

with

$$\psi(t) = a(t)K^0 + b(t)\bar{K}^0,$$

where Γ is the 2×2 unitary decay matrix and M is the corresponding unitary mass matrix. The matrix elements as related to the weak-interaction Hamiltonian have been given by many authors[6–7] and will not be reproduced here.

Keeping the (mass-decay) matrix in a general form to allow for the possibility of external fields or *CPT* violation, one can write

$$-\frac{d}{dt}\begin{pmatrix} a \\ b \end{pmatrix} = \begin{pmatrix} R & p^2 \\ q^2 & S \end{pmatrix}\begin{pmatrix} a \\ b \end{pmatrix}, \tag{2}$$

which has eigenvalues

$$\Gamma_{1,2} = \frac{R+S}{2} \pm \left[\left(\frac{R-S}{2}\right)^2 + p^2q^2\right]^{1/2}$$

and eigenvectors $|K_1^0\rangle$ and $|K_2^0\rangle$. When $R = S$, these reduce to the familiar results derived first by Lee *et al.*[5] For any initial state of the K^0-$\bar{K}^0$ system characterized by

$$\psi(0) = \begin{pmatrix} a(0) \\ b(0) \end{pmatrix},$$

there exist standing-wave solutions to the interaction equation such that

$$\psi(t) = \begin{pmatrix} A \\ B \end{pmatrix} e^{-\Gamma_1 t} + \begin{pmatrix} C \\ D \end{pmatrix} e^{-\Gamma_2 t},$$

with

$$\begin{aligned} A &= [(\Gamma_1 - S)a(0) + p^2 b(0)]/(\Gamma_1 - \Gamma_2), \\ B &= [q^2 a(0) + (\Gamma_1 - R)b(0)]/(\Gamma_1 - \Gamma_2), \\ C &= [(\Gamma_1 - R)a(0) - p^2 b(0)]/(\Gamma_1 - \Gamma_2), \\ D &= [-q^2 a(0) + (\Gamma_1 - S)b(0)]/(\Gamma_1 - \Gamma_2). \end{aligned} \tag{3}$$

The $\Gamma_{1,2}$ are, of course, identified with the mass and lifetime of $K_{1,2}$, viz.,

$$\Gamma_1 = iM_1 + (1/2\tau_1) \quad \text{and} \quad \Gamma_2 = iM_2 + (1/2\tau_2).$$

We further note that if $(R-S) \ll pq$, then $2pq \cong \Gamma_1 - \Gamma_2$.

For a discussion of the consequences of *CPT* noninvariance, see Refs. 6 and 8. This discussion is re-

* Research supported largely by the U. S. Office of Naval Research Contract No. N0014-67-A-0151-0001.
† Now with the Commission on College Physics, Ann Arbor, Michigan.
‡ National Science Foundation predoctoral fellow, 1962–65.
§ Present address: University of California, San Diego, La Jolla, California. National Science Foundation cooperative fellow, 1964–65 and Minnesota Mining and Manufacturing Company postdoctoral fellow, 1965–66.
[1] J. Christenson, J. Cronin, V. Fitch, and R. Turlay, Phys. Rev. Letters **13**, 138 (1964); A. Abashian, R. Abrams, D. Carpenter, G. Fisher, B. Nefkens, and J. Smith, *ibid.* **13**, 243 (1964).
[2] W. Vernon, R. Roth, and J. Russ, Bull. Am. Phys. Soc. **10**, 466 (1965).
[3] V. Fitch, R. Roth, J. Russ, and W. Vernon, Phys. Rev. Letters **15**, 73 (1965). We have changed the notation from that used in this preliminary report to correspond to that which is now generally accepted. In particular, we have reverted to calling the observed particles K_1^0 and K_2^0 since there is no longer any need to reserve this notation for the eigenstates of *CP*.
[4] J. Russ, V. Fitch, R. Roth, and W. Vernon, Bull. Am. Phys. Soc. **11**, 341 (1966).
[5] T. D. Lee, R. Oehme, and C. N. Yang, Phys. Rev. **106**, 340 (1957).
[6] R. G. Sachs, Ann. Phys. (N. Y.) **22**, 239 (1963).
[7] L. B. Okun, Ann. Rev. Nucl. Sci. **9**, 61 (1959).
[8] T. D. Lee and C. S. Wu, Ann. Rev. Nucl. Sci. **16**, 511 (1966).

stricted to the case of CPT invariance.[6,8] Then if the transition amplitude for $K^0 \to \pi\pi$ in isotopic spin state T is A_T, the corresponding amplitude for $\bar{K}^0 \to \pi\pi$ is A_T^*. Hence the time-dependent $\pi^+\pi^-$ amplitude from the K-$\bar{K}$ system is

$$A_{\pi^+\pi^-}(t) = \frac{e^{-\Gamma_1 t}}{\sqrt{3}}[A(\sqrt{2}A_0 + FA_2) + B(\sqrt{2}A_0^* + FA_2^*)]$$
$$+ \frac{e^{-\Gamma_2 t}}{\sqrt{3}}[C(\sqrt{2}A_0 + FA_2) + D(\sqrt{2}A_0^* + FA_2^*)] \quad (4)$$

for $F = e^{i(\delta_2 - \delta_0)}$ and δ_T the $\pi\pi$ final-state scattering phase shift for isotopic spin T at $E_{\pi\pi} = m_K$. The initial boundary conditions are included in A, B, C, and D. The relative phase of K^0 and $\bar{K}^0$ and of the amplitudes A_T can be chosen at will, but the most widely used choice is to make A_0 real and K^0 and $\bar{K}^0$ relatively real. Using Eq. (4) and noting that $|A_2| \ll |A_0|$, as known from K^+ and K_1^0 decays, one finds for the ratio of the long-lived to short-lived $\pi^+\pi^-$ amplitudes from a K^0 initial state

$$N_{+-} = -\frac{R-S}{(p+q)^2} + \frac{p-q}{p+q} + \frac{iF}{\sqrt{2}} \mathrm{Im}\frac{A_2}{A_0} \quad (5)$$

to lowest order in $(R-S)/pq$. Three particular cases are of interest here.

Case I. The 2π decay of the K_2 is caused by an external cosmological field as exemplified by those proposed in Ref. 9. Only the first term of N_{+-} contributes and $R-S$ is equal to some potential which has an energy dependence given by E^J where J is the (integer) spin of the field quanta.

Case II. CP violation with no material and no external field. Here $R-S=0$ and one has

$$N_{+-} = \epsilon + \epsilon' = \eta_{+-},$$

with

$$\epsilon = \frac{(p-q)}{(p+q)} \quad \text{and} \quad \epsilon' = \frac{iF}{\sqrt{2}} \mathrm{Im}\frac{A_2}{A_0}. \quad (6)$$

Wolfenstein[10] and Gürsey and Pais (unpublished) have suggested that the CP violation be due to a new interaction which causes direct $K^0 \leftrightarrow \bar{K}^0$ transitions. This would appear in the off-diagonal elements and hence in ϵ.

Case III. CP violation as described by Case II coupled with scattering of the K^0 and $\bar{K}^0$ in the medium leads to

$$R-S = 2\pi i[f(0) - \bar{f}(0)]Nc^2 p_K/(km_K c^2),$$

where $f(0)$ and $\bar{f}(0)$ are the forward scattering amplitudes for the K^0 and $\bar{K}^0$, respectively, N is the number of scattering centers per unit volume, and k is the wave number. The transformation from the laboratory to the c.m. system leads to the factor $cp_K/m_K c^2$. With CP violation and material present, the equilibrium amplitude ratio is

$$N_{+-} = \eta_{+-} + A_r,$$

where the regeneration amplitude A_r is given by

$$A_r = \pi i[f(0) - \bar{f}(0)]N\Lambda/k(i\delta + \tfrac{1}{2})$$
$$= 2\pi i f_{21}(0)N\Lambda/k(i\delta + \tfrac{1}{2}), \quad (7)$$

with Λ equal to the mean decay length of the K_1^0 and $\delta = (m_1 - m_2)c\tau_1/\hbar$. The $\pi^+\pi^-$ intensity in a material medium is proportional to $|N_{+-}|^2$, providing the short-lived components have been allowed to decay away. Then the $\pi^+\pi^-$ decay rate is

$$I_{\pi^+\pi^-} \propto |A_r + \eta_{+-}|^2 = |A_r|^2 + |\eta_{+-}|^2$$
$$+ 2|A_r||\eta_{+-}| \cos\alpha, \quad (8)$$

where α is the phase difference between A_r and η_{+-}. The phase of A_r is, in principle, known and a measurement of the interference angle α will yield information about the phase of η_{+-}.[3,11]

We note that A_r is a linear function of the density. By measuring the $\pi^+\pi^-$ event rate in a prescribed region of space as a function of the density of the scattering material (regenerator) one can obtain for m different densities, $|A_r|$, $|\eta_{+-}|$, and $\cos\alpha$, subject to $m-3$ constraints. The results are independent of the apparatus detection efficiency and require only that it be constant. The maximum interference effects occur when $|A_r| \cong |\eta_{+-}|$. This occurs in Be when its density is approximately 0.1 g/cm^3.

From the relations above it is easily shown that with a K_2^0 beam incident on a piece of material of thickness L, the $\pi^+\pi^-$ amplitude as a function of distance x behind the material is, to a good approximation, given by

$$A_{+-}(x) \propto \eta_{+-} + A_r(1 - e^{-(i\delta + \frac{1}{2})L})e^{-(i\delta + \frac{1}{2})x}, \quad (9)$$

with both L and x measured in units of the mean decay length of the K_1^0. The observation of the spatial dependence of the interference was originally discussed by Whatley[12] and Sachs[6] as a test of T noninvari-

[9] J. Bell and J. Perring, Phys. Rev. Letters **13**, 348 (1964); J. Bernstein, N. Cabibbo, and T. D. Lee, Phys. Letters **12**, 146 (1964); J. Bernstein, G. Feinberg, and T. D. Lee, Phys. Rev. **139**, B1650 (1965); T. D. Lee, Phys. Rev. **137**, B1621 (1965); S. Weinberg, Phys. Rev. Letters **13**, 495 (1964); B. Ioffe and M. Terent'ev, Zh. Eskperim. i Teor. Fiz. **47**, 744 (1965) [English transl.: Soviet Phys.—JETP **20**, 496 (1965)].

[10] L. Wolfenstein, Phys. Rev. Letters **13**, 562 (1964).

[11] A. Firestone, J. Kim, J. Lach, J. Sandweiss, H. Taft, V. Barnes, H. Foelsche, T. Morris, Y. Oren, and M. Webster, Phys. Rev. Letters **16**, 556 (1966).

[12] M. Whatley, Phys. Rev. Letters **9**, 317 (1962).

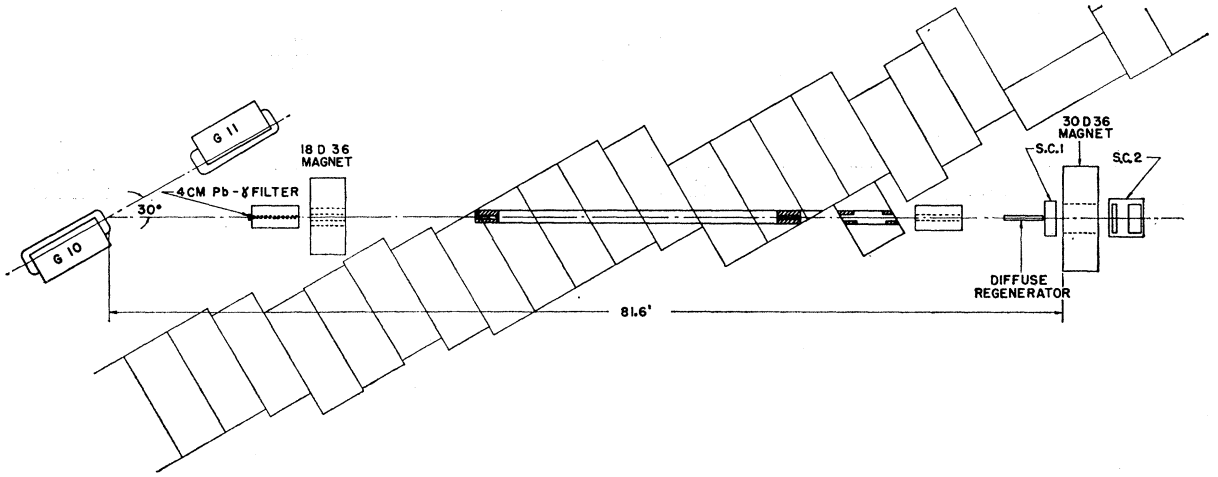

FIG. 1. Plan view of the experimental setup with the diffuse regenerator in place. The apparatus was unaltered when other targets were substituted for the diffuse regenerator.

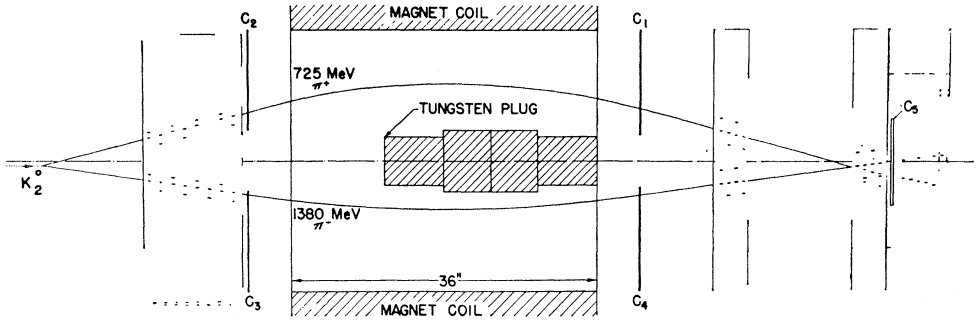

FIG. 2. Spark-chamber photographs of a labeled $K_2^0 \to \pi^+ + \pi^-$ decay, including outline drawings of the magnet aperture and trigger counters. The pion momenta are labeled and the K_2^0 vector direction indicated.

ance and has been successfully exploited in other experiments.[13–15]

II. EXPERIMENTAL ARRANGEMENT

As has been emphasized in the past,[1] the relatively rare $\pi^+\pi^-$ decay modes of the K_2^0 meson can be selected from the normal three-body decays by a sufficiently accurate momentum analysis of each of the two charged products. Therefore the main experimental requirement, in addition to a beam of neutral K mesons, is a magnetic spectrometer tailored for the best compromise between high resolution and large acceptance and which, ideally, selects two-body decays preferentially.

Figure 1 shows a plan view of the beam and spectrometer arrangement at the Brookhaven alternating-gradient synchrotron. Incident protons at 29 GeV struck an internal beryllium-wire target 0.04 in. in diameter extending 0.5 in. along the proton orbit. The secondary beam was defined at an angle of 30° to the protons by a collimator having an aperture 4×4 in. ending 70 ft from the target. This was 55 in. ($15K_1^0$ mean lives at 1.5 GeV/c) in front of the region from which K_2^0 decays were accepted. A second collimator with a 1×2-in. aperture 15.5 ft from the target and a charged-particle sweeping magnet having a field integral of 600 kG in. completed the beam. The γ rays were largely removed by eight radiation lengths of lead between the target and the first collimator. It was estimated that neutrons made up 80 to 90% of the beam, and they were sampled by a counter telescope comprised of three thin scintillation counters 16.5 ft in front of the decay region. Triple-coincidence pulses from proton recoils in the first detector were counted and used for monitoring purposes.

The spectrometer for detecting V decays of neutral particles consisted of thin-foil spark chambers for track delineation before and after a "picture frame" magnet. Figure 2 shows the layout of the chambers and magnetic field region in the horizontal plane and shows a sample event, with spark-chamber photographs superposed on a line drawing of the magnet. The front spark chamber

[13] C. Alff-Steinberger, W. Heuer, K. Kleinknecht, C. Rubbia, A. Scribano, J. Steinberger, M. Tannenbaum, and K. Tittel, Phys. Letters **20**, 207 (1966); **21**, 595 (1966).

[14] M. Bott-Bodenhausen, X. DeBouard, D. Cassel, D. Dekkers, R. Felst, R. Mermod, I. Savin, P. Scharff, M. Vivargent, T. Willitts, and K. Winter, Phys. Letters **20**, 212 (1966); **23**, 277 (1966).

[15] R. E. Mischke, A. Abashian, R. J. Abrams, D. W. Carpenter, B. M. K. Nefkens, J. H. Smith, R. C. Thatcher, L. J. Verhey, and A. Wattenberg, Phys. Rev. Letters **18**, 138 (1967).

had eight $\frac{3}{8}$-in. gaps in an active volume 10 in. in the beam direction, 8 in. high, and 24 in. wide, ending 24.5 in. from the center of the magnet. The rear chamber was made of two sets of four $\frac{3}{8}$-in. gaps each with a volume 3 in. along the beam, 13 in. high, and 28 in. wide, with the nearest set beginning 32.5 in. from the magnet center. A 13-in.-long region separated the two banks. The thin plates in both chambers were constructed by gluing 0.001-in. aluminum foil to rigid aluminum frames. The thin plates in the rear chamber were followed by a set of six plates, each containing one-half of a radiation length of Pb for electron identification.

The magnet field was 6 in. high, 29 in. wide, and 36 in. along the beam; its magnetic field integral along the beam axis was 486.1 ± 0.75 kG in. To the extent that the field integral is constant across the aperture (true to better than 0.15%) the spectrometer can be characterized by

$$\Delta P_t = P_t(\text{in}) - P_t(\text{out}) = 370.2 \text{ MeV}/c,$$

where P_t is the transverse momentum in the plane perpendicular to the magnetic field direction. If two charged particles enter the field with equal transverse momenta, they emerge with equal transverse components, and further, if $\Delta P_t = 2P_t(\text{in})$, the trajectories are mirror images of each other before and after the magnet. Taking the kaon direction as the axis which is used to define P_t, for two-body decay one sees that the crossing point of the trajectories beyond the magnet, as projected on the horizontal plane, lies on the horizontally projected kaon trajectory. The effect can be observed in Fig. 2. This feature results in a large increase in resolution for the measured direction of the K_2^0 and insensitivity of the reconstructed invariant mass to measurement errors in the front spark chamber.

The chambers were photographed through spherical Lucite field lenses mounted immediately above each chamber. Redundant stereo views of the front chamber were provided by a single side-view mirror, and by 10° stereo images of tracks obtained by inserting $\frac{1}{4}\times\frac{3}{8}\times 28$-in. strip mirrors at alternating 5° angles beneath all the gaps. Fiducial marks consisting of lines scribed on Lucite plates and edge lighted by xenon flash tubes outlined the top views. True space positions were obtained from another set of fiducial lines scribed on Lucite plates covering three sides of the chambers and from scratches on the front surfaced strip mirrors. Decay products were detected by four counters placed at the entrance and exit of the magnet. These were $6\times 15\times\frac{1}{8}$-in. plastic scintillators with 25-in.-long light pipes and covered the full aperture of the magnet with the exception of the 4-in.-wide beam region. A pulse from a fifth scintillation counter centered in the rear spark chamber was part of the coincidence requirement for most of the data.

Various configurations of material in the "decay volume" were used and these are illustrated in Fig. 3. Configuration A yielded all the data on $K_2^0 \to \pi^+ + \pi^-$ free decay rates; about $\frac{1}{4}$ of this data was taken with a vacuum tank at a pressure of 5×10^{-4} atm in the decay region. The first part of the free-decay data and all of the tungsten regeneration data (configuration B) were taken with a four-counter trigger requirement. All other configurations utilized a five-counter trigger scheme which discriminated against neutron-induced background. In configuration B the regenerator, followed by an anticoincidence counter, was moved along the beam line in 4-in. steps to provide coherently regenerated K_1^0 whose $\pi^+\pi^-$ decays were used as an apparatus (detection efficiency) calibration. In configurations C and D, the regenerator density was varied by changing the spacing and orientation of thin beryllium plates.

The average event rate for configuration A under the running conditions of this experiment was about 4/h. To minimize machine-dependent fluctuations, the various configurations involving material in the beams were alternated with free decay every few hours.

There was no unique characteristic of the $K_{\pi 2}$ decays adequate to identify them by inspection, and 70% of the pictures satisfied all scanning criteria and were measured on an angular encoding machine. The event selection efficiency of the scanners was greater than 95%, and the standard deviation of an angular measurement was ~ 3 mrad. A particle was labeled as an electron if its track showed at least two extra sparks near to but distinct from the main track in the shower chamber. The field integral was evaluated by a numerical integration from a set of field measurements made with a Rawson rotating-coil gaussmeter and the

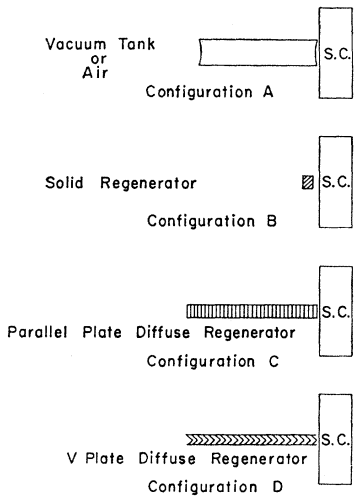

FIG. 3. Schematic representation of the targets put into the K_2^0 beam during the experiment. In A, K_2^0 decays in air or vacuum were observed. In B, K_1^0 decays behind a single slab of regenerator were measured. In C, $\pi^+\pi^-$ pairs emanating from within a set of thin Be plates were observed. For D, the plates from C were rearranged in a V pattern intercepting a 1-in. bite in the horizontal plane.

central field value as determined from a nuclear-magnetic-resonance probe. For that data involving material in the beam, corrections were made to the total momentum of each particle for ionization loss in the scatterer. The momentum-dependent corrections shifted the momenta, masses, and angles by less than 1%.

To separate the 2π events from the background, one assumes a two-pion decay and calculates the vector momentum $\mathbf{p}$ of the K_2^0 and the effective mass m^* from the relations

$$\mathbf{p}=\mathbf{p}_1+\mathbf{p}_2,$$
$$(m^*)^2=2(m_\pi^2+E_1E_2-\mathbf{p}_1\cdot\mathbf{p}_2),$$

where $\mathbf{p}_1$ and $\mathbf{p}_2$ are the reconstructed vector momenta of the charged secondaries, E_1 and E_2 their energies. One gains most in the suppression of background by restricting the angle θ between the beam direction and vector $\mathbf{p}$. Two-body events plotted in a $\cos\theta$ distribution must appear at $\cos\theta=1$ within the resolution. The transverse-momentum requirement imposed by the spectrometer made it extremely insensitive to 3π decays. The three-body leptonic decay modes K_{l3} have no preferred value of the transverse momentum for the charged prongs and give a smoothly varying background in this distribution.

For all the data the background in the angular distribution for events having $0.9940<\cos\theta<0.9999$ can be fit well by an exponential distribution in $\cos\theta$. The events arising from the allowed decay region and having m^* between 487 and 507 MeV are plotted as a function of $\cos\theta$. An example is given in Fig. 4. The 2π events show up as a pronounced peak in the region $\cos\theta>0.99990$. The background under the peak is calculated by fitting an exponential to the events outside the 2π peak and then extrapolating the background curve under the peak. In the regeneration studies the density of the scattering medium was held below the level where degradation of the resolution in the m^* and $\cos\theta$ distributions due to multiple Coulomb scattering of the pions would affect the results. The fact that the spectrometer responds in precisely the same way to $\pi^+\pi^-$ pairs from coherently regenerated K_1^0 and from K_2^0 decay is shown in Fig. 5. Figure 6 shows the mass distribution for events in the forward direction. We obtain $m(K_1^0)=497.44\pm0.50$ MeV.

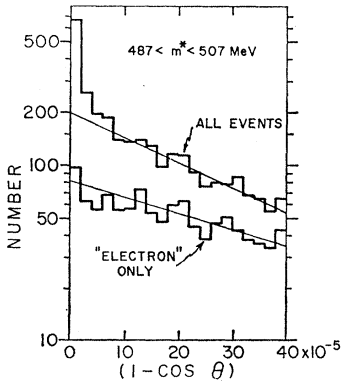

FIG. 4. Angular distribution for K_2^0 decay showing leptonic background and forward peak from $K_2^0 \to \pi^+\pi^-$. Events shown have effective masses of 497 ± 10 MeV, assuming that all are $\pi^+\pi^-$ decays. The upper curve includes all events. The lower curve includes only events identified as K_{e3} decays from electron showers. The absence of any forward peak for the latter events indicates that no true $\pi^+\pi^-$ decays are mislabeled as K_{e3}.

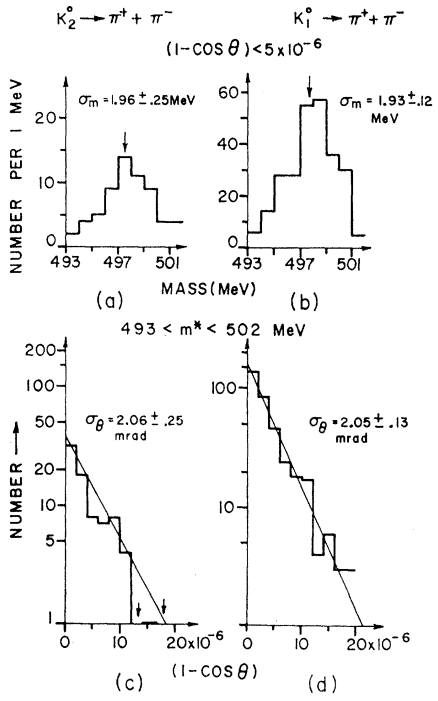

FIG. 5. Comparison of effective mass and angular distributions for selected events from $K_2^0 \to \pi^+ + \pi^-$ and $K_1^0 \to \pi^+ + \pi^-$ as measured in this spectrometer. The $K_2^0 \to \pi^+ + \pi^-$ come from free decay, and the $K_1^0 \to \pi - + \pi^-$ from coherent regeneration.

III. FREE-DECAY BRANCHING RATIO

The branching ratio for $\pi^+\pi^-$ decay was determined from the numbers of two- and three-body decays detected in the apparatus with the relative detection

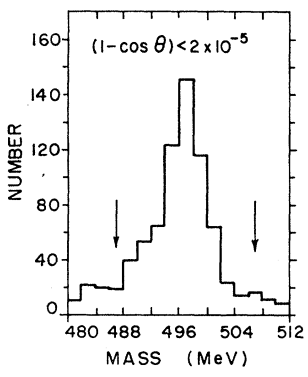

FIG. 6. Distribution of effective masses for all events having reconstructed K angles <4.5 mrad from the forward direction. The arrows indicate the mass cuts used in the final event selection.

efficiences taken into account. The relative detection efficiencies depend on the K_2^0 momentum spectrum, the K_{l3} decay properties, and the apparatus acceptance.

To compute the detection efficiency, pseudo $K_2^0 \rightarrow 2\pi$ events were generated on a computer at a fixed K-meson momentum. The pion trajectories were required to pass all the spectrometer apertures, counters, spark-chamber fiducial limits, and scanning criteria. The resulting efficiency from the Monte Carlo calculations $\epsilon_{2\pi}(P)$ is given in Table I.

For K_{l3} decays one measures only the "visible momentum"

$$\mathbf{P}'=\mathbf{p}_\pi+\mathbf{p}_l=\mathbf{P}-\mathbf{p}_\nu$$

rather than P. Therefore it is necessary to calculate $\epsilon_l(P,P')$, the efficiency for detecting a leptonic event with K_2^0 momentum P and observed momentum P'. The actual calculation was performed separately for K_{e3} and $K_{\mu 3}$, and the results were added with the weighting:

$$\epsilon_l(P,P')=0.58\epsilon_{e3}(P,P')+0.42\epsilon_{\mu 3}(P,P').$$

The pion and lepton energies in the K_2^0 rest frame were selected randomly according to a Dalitz-plot density $D(E_\pi,E_l)$ discussed by MacDowell,[16] using a pure-vector interaction with real, energy-independent form factors f_1 and f_2. We used $f_1/f_2=0.85$ but the result is not sensitive to this ratio.[17]

$\epsilon_l(P,P')$ can be written as a 12×12 matrix (see Table II) whose entries represent the average efficiency over 200 MeV/c wide intervals in both P and P'. If $\mathbf{S}$ and $\mathbf{S}'$ are column and row vectors representing the corresponding averages of the P and P' spectra, then a formal solution of the set of linear equations $\epsilon_l\mathbf{S}=\mathbf{S}'$ yields $\mathbf{S}$, the spectrum of particles decaying in front of the apparatus. Correcting for decays, we found that a Cocconi spectrum[18] $F(P)=A_0Pe^{-P/2P_0}$ fits the production spectrum with $P_0=0.19$ GeV/c and normalization $A_0\approx 0.040\pm 0.015$ K_2^0/proton sr (GeV/c). The production spectrum is plotted in Fig. 7.

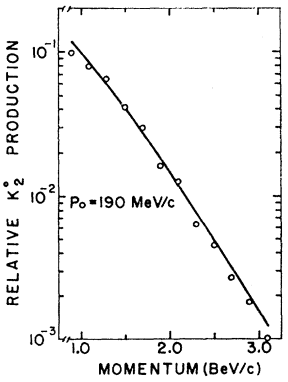

FIG. 7. Production spectrum for K_2^0 mesons at 30° at the AGS, as reconstructed from observed K_{e3} and $K_{\mu 3}$ decays. The solid curve is a Cocconi spectrum.

$S(p)=A_0pe^{-p/2p_0}$ for $p=0.19$ GeV/c

and

$A_0=0.04\pm 0.015$ K_2^0/proton sr (GeV/c).

[16] S. W. MacDowell, Nuovo Cimento **6**, 1445 (1957).
[17] G. Jensen, F. Shaklee, B. Roe, and D. Sinclair, Phys. Rev. **136**, B1431 (1964).
[18] G. Cocconi, University of California Radiation Laboratory Report No. UCRL-10022, p. 167 (unpublished).

TABLE I. $K_{\pi 2}$ branching ratio data.

Kaon momentum (GeV/c)	Total number in "$K_{\pi 2}$"	K_{l3} in "$K_{\pi 2}$" (background)	$K_{\pi 2}$	Detection efficiency $\epsilon_{\pi 2}$ (%)
0.8–1.2	195±14	55±7	140±16	0.172
1.2–1.6	273±17	128±8	145±18	0.437
1.6–2.0	243±16	109±7	134±17	0.762
2.0–2.4	151±12	77±8	74±15	1.130
2.4–2.8	67±8	37±6	30±10	1.442

For $0.8<P<2.8$ GeV/c, the momentum-averaged ratio was found to be $\langle\epsilon_{\pi 2}\rangle/\langle\epsilon_{l3}\rangle=12.2$. The $K_{\pi 2}$ decays in this interval were summed and an average branching ratio calculated using the observed K_{l3} decays restricted to the same interval in P'. From 525±33 $K_{\pi 2}$ decays the *uncorrected* branching ratio of $K_{\pi 2}$ to leptonic modes is $(2.04\pm 0.15)\times 10^{-3}$. This ratio is increased by 9% because of event loss through pion decay, 1% because of pion absorption in gas, chamber plates, and counters, 3% due to measurement errors, and 1% from the estimated number of K_{l3} events which were really neutron-produced stars in the air in the decay region. The total correction is 14±3%. Using the ratio

$$\Gamma(K_{l3})/\Gamma(\text{all charged modes})=0.84\pm 0.02,$$

we obtain a branching ratio, averaged over the momentum interval 0.8 to 2.8 BeV/c,

$$\Gamma(\pi^+\pi^-)/\Gamma(\text{all charged modes})=(1.97\pm 0.16)\times 10^{-3}.$$

A possible momentum dependence of the branching ratio was investigated by finding the relative branching ratio in 400-MeV/c intervals over the range 0.8 to 2.8 GeV/c and the results are shown in Fig. 8(a). The five data points were fit to a function $R_0\gamma^n$ where γ is the energy of the K meson. The χ^2 fit is shown in Fig. 9(a). The result is $n=0.03\pm 0.33$.

Another check on a momentum dependence of the decay to 2π is provided by a comparison of the free decay with the 2π from coherent regeneration. The relative intensity of K_1^0 behind a piece of material is

TABLE II. Percentage acceptance $\epsilon_l(P,P')$ of K_{l3} events with incident momentum P and observed momentum P'. $P=0.7+0.2i$ GeV/c; $P'=0.7+0.2j$ GeV/c. Multiply entries by 10^{-4} to get percent. Average error in a single entry is ~15% off-diagonal, ~8% on-diagonal.

j \ i	1	2	3	4	5	6	7	8	9	10	11	12
1	31	29	7	0	0	0	0	0	0	0	0	0
2	0	80	80	41	13	8	0	0	0	0	0	0
3	0	0	172	142	71	40	38	22	0	0	0	0
4	0	0	0	274	235	136	95	45	30	13	0	0
5	0	0	0	0	350	380	208	133	98	80	50	0
6	0	0	0	0	0	382	505	343	202	180	170	110
7	0	0	0	0	0	0	473	526	312	147	156	96
8	0	0	0	0	0	0	0	467	639	397	290	97
9	0	0	0	0	0	0	0	0	417	572	510	266
10	0	0	0	0	0	0	0	0	0	450	505	460
11	0	0	0	0	0	0	0	0	0	0	436	855
12	0	0	0	0	0	0	0	0	0	0	0	475

given by the absolute square of Eq. (9). For thin samples this intensity is insensitive to the K_1-K_2 mass difference and sensitive only to $|f(0)-\bar{f}(0)|/2 = |f_{21}(0)|$. Figure 8(b) shows R as determined from a comparison of $\pi^+\pi^-$ rates from coherently regenerated K_1^0 and K_2^0 decay. The regeneration amplitudes were calculated from an optical model as a function of momentum, assuming no real parts in the scattering amplitudes. Adding reasonable real parts has a negligible effect on the magnitude of the regeneration amplitude. Since the regeneration data were taken with the regeneration material successively moved to different positions throughout the decay volume, the relative detection efficiencies for regeneration and free decay were made equal.

IV. NEUTRAL CURRENTS

A search was carried out for $K_2^0 \to \mu^+ + \mu^-$ and $K_2^0 \to \mu^\pm + e^\mp$, which are signatures of neutral currents in the weak interactions. Figure 10(a) shows the invariant-mass plot for free-decay events in the forward direction assuming $\mu^+\mu^-$ decay. The peak at 460 MeV is due to $\pi^+\pi^-$ events. Events in a 6-MeV region about the K_2^0 mass are plotted in Fig. 10(b) as a function of the direction cosine for this assumption; Fig. 10(c) shows the equivalent plot assuming a $\pi^+\pi^-$ decay. In these plots, events having one secondary labeled as an electron were not used. There is no evidence of any enhancement in the direction-cosine plot for $\mu^+\mu^-$, and we place a limit on the number of events with $(1-\cos\theta) < 10^{-5}$ at $N_{\mu\mu} \leq 4$. Since this same interval in the $K_2^0 \to$

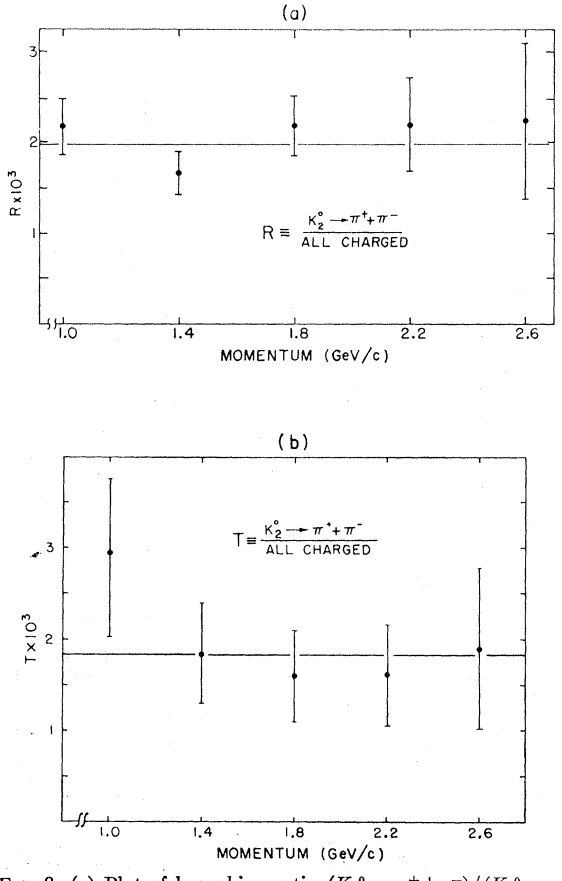

FIG. 8. (a) Plot of branching ratio $(K_2^0 \to \pi^+ + \pi^-)/(K_2^0 \to$ all charged modes) as a function of momentum. The χ^2 for a fit to a constant branching ratio is 2.5 for 4 degrees of freedom, and the branching ratio is $(1.97\pm0.16)\times10^{-3}$. (b) Branching ratio for $(K_2^0 \to \pi^+ + \pi^-)/(K_2^0 \to$ all charged modes) as a function of momentum as determined by comparison with coherent regeneration. Again a constant fits the data well, and the branching ratio here is $(1.82\pm0.33)\times10^{-3}$, in good agreement with the preceding result.

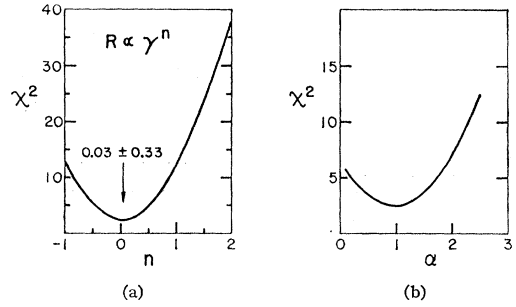

FIG. 9. (a) Results of a χ^2 fit of a branching ratio R varying as γ^n to the data from free K_2^0 decay. The fit predicts the exponent $n=0.03\pm0.33$, consistent with zero. The probability that $n=2$ for the data is 1 part in 10^6. (b) Results of a χ^2 fit to the total decay rate of a new neutral K meson allowed to decay via the $\pi^+\pi^-$ mode and having the same production spectrum as K_2^0. The curve plotted is χ^2 versus the ratio $\alpha=\Gamma_X/\Gamma_{K_2^0}$. The result is $\Gamma_X/\Gamma_{K_2^0}=1.02\pm0.60$.

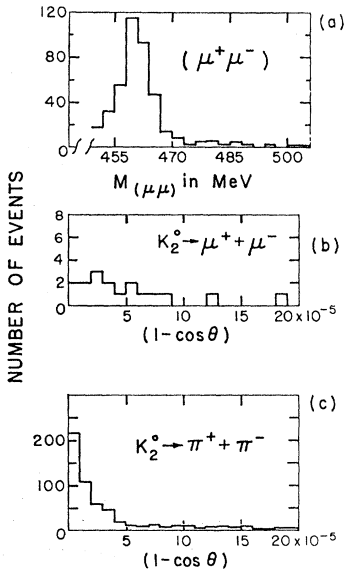

FIG. 10. (a) Invariant mass distribution assuming a decay $K_2^0 \to \mu^+ + \mu^-$. The absence of any enhancement in the K-mass region limits the branching ratio $\Gamma(K_2^0 \to \mu^+ + \mu^-)/\Gamma(K_2^0 \to$ all charged modes) $<3.5\times10^{-5}$ with 90% confidence. (b) Angular distribution for events with an invariant mass of 497 ± 3 MeV, assuming a decay $K_2^0 \to \mu^+ + \mu^-$. As in (a) there is no evidence for this decay mode. (c) Angular distribution assuming $K_2^0 \to \pi^+ + \pi^-$ for invariant mass of 497 ± 3, for comparison with (b).

$\pi^+ + \pi^-$ case yields 230 events, we have

$$R(K_2^0 \to \mu^+ + \mu^-)/R(K_2^0 \to \text{all charged}) \leq 3.5 \times 10^{-5} \quad (90\% \text{ confidence}).$$

In the case of $\mu^\pm e^\mp$ only the identified electron events were used. Therefore the μ and e tracks were labeled in constructing the invariant mass of the system. There were no events in a broad region of mass and $\cos\theta$ under these conditions so that a limit of ~ 2 possible events was set, including effects of a 75% electron detection efficiency. Hence the limits we find for the $K_2^0 \to \mu^\pm + e^\mp$ relative rate at the 90% confidence level are

$$R(K_2^0 \to \mu^\pm + e^\mp)/R(K_2^0 \to \text{all charged}) \leq 8 \times 10^{-6}$$

or

$$R(K_2^0 \to \mu^\pm + e^\mp)/R(K^+ \to \mu^+ + \nu) \leq 2.2 \times 10^{-6}.$$

V. INTERFERENCE

As discussed in the Introduction, the interference between the amplitude for free decay to $\pi^+\pi^-$ and the $\pi^+\pi^-$ amplitude from coherent regeneration was observed by varying the average density of the regeneration material in the decay region. Beryllium was selected as the regenerator to minimize the multiple Coulomb scattering of the charged pions as they exited from the material. The Be was in the form of solid plates each $4 \times 7 \times 0.022$ in. and the density was varied by changing the average spacing of the plates along the beam direction. Maximum interference effects are expected when $|A_r| \cong |\eta_{+-}|$ and from previous measurements[19] it was known that this could be effected by a Be regenerator having a density of 0.10 g/cm^3, corresponding to a plate spacing of 0.378 in. Measurements were made at densities of 0, 0.05, 0.10, and 0.40 g/cm^3. The Be regenerator extended 40 in. along the K_2^0 beam. However, the origins of the events used in the analysis were restricted to the final 18 in., thereby allowing 22 in. (or ~ 7 K_1^0 decay lengths at the mean momentum of 1.6 GeV/c) for the beam composition to come to equilibrium. The width of the 0.4-g/cm^3 regenerator was decreased from 4 to 1 in. to reduce the total amount of material traversed by the charged pions. This was accomplished by arranging the plates in a V pattern with a gap of 0.75 in. between adjacent plates; see Fig. 3. The efficiency of the apparatus varies only slightly in the transverse dimension and these results are scaled to the standard 4 in. width with good precision. Further data were taken with the density at 0.15 g/cm but with the length of the regenerator along the beam set at 30 sec of arc. Because of the different length these data were used only as a consistency check, not in the final determination of the phase angle.

[19] J. Christenson, J. Cronin, V. Fitch, and R. Turlay, Phys. Rev. 140, B74 (1965).

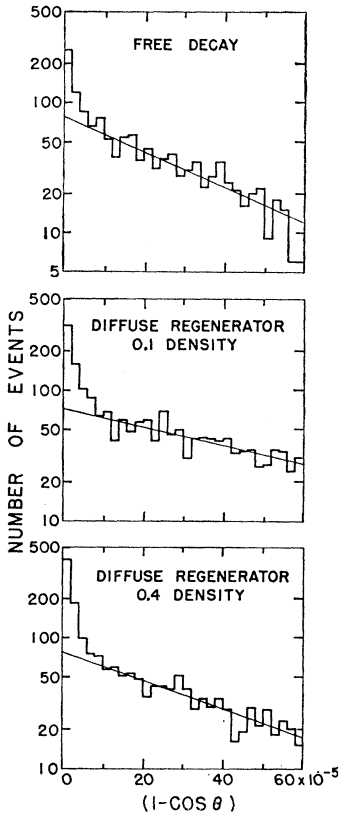

FIG. 11. Angular distributions for events having invariant masses of 497±10 MeV from free decay and diffuse regenerators of density 0.1 and 0.4 g/cm^3. The increased width of the peaks for the regenerator distributions is due to multiple Coulomb scattering of the pions in the regenerator material.

Typical data are shown in Figs. 11 and 12. The events selected in the various experimental configurations originate in the same spatial region and the result is correspondingly insensitive to detection characteristics and efficiency. However, corrections to the data must be made for the attenuation of the K_2^0 and $\pi^\pm$ mesons in the regenerator. For these corrections a total cross section of 273±15 mb was used for $\pi^\pm$ and 192±5 mb for the K_2^0.[20] The formulas developed in the Intro-

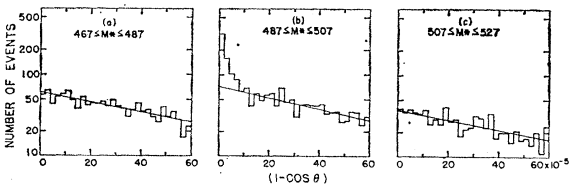

FIG. 12. Angular distributions for events from the 0.1 regenerator for three bands of invariant mass: (a) 477±10 MeV; (b) 497±10 MeV; (c) 517±10 MeV. The good straight-line fit to the data in (a) and (c) supports its use in evaluating the background under the forward peak in (b).

[20] The pion cross sections are from J. Cronin, R. Cool, and A. Abashian, Phys. Rev. 107, 1121 (1957). The K^+ and K^- cross sections, from which we have estimated the corresponding K^0-$\bar{K}^0$ cross sections, have been measured for us by the group of Cool *et al.* at 1.55 and 1.75 GeV/c.

duction apply to a continuous media. The maximum correction due to the granular nature of the regenerator was less than 1%. Corrections for the end effects of the regenerator are less than 4%.

The corrected data from runs at the four densities were fitted to the function

$$R_i = T(1+d_i^2F^2+2d_iF\cos\alpha), \qquad (10)$$

where R_i is the measured rate from the ith density regenerator, $F=|A_r|/|\eta_{+-}|$ with the magnitude of A_r evaluated at a standard density of 0.1 g/cm³ and d_i is the density in units of the standard density. The normalization factor T is proportional to the free-decay rate. The result of the fitting is shown in Fig. 13 with $\cos\alpha=1$, 0, and -1, corresponding to fully constructive interference, no interference, and fully destructive interference. Figure 14 shows the two-dimensional χ^2

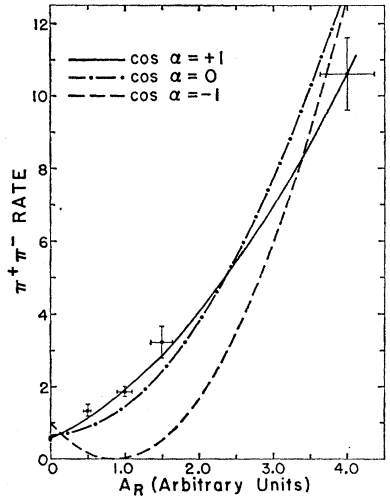

FIG. 13. Measured event rate as a function of regeneration amplitude. The solid curves are the results of best χ^2 fits to the data for interference angles of 0, $\pi/2$, and π. Only the curve for 0 angle gives a good fit to the data.

plot with the minimum of 1.88 for 1 degree of freedom, and the one standard deviation and 90% confidence level contours. Integrating over the surface to remove the F dependence, we find

$$\cos\alpha=1.00\pm0.21.$$

Likewise, integrating to remove the $\cos\alpha$ dependence we obtain

$$F=0.86\pm0.08.$$

We emphasize that these results are independent of the sign and magnitude of the K_1-K_2 mass difference.

Using the value of F obtained here and $\eta_{+-}=1.91\times10^{-3}$, we compute $|f_{21}(0)|$ to be

$$|f_{21}(0)|=2.68\pm0.27\ \text{F}$$

for a mass difference $\delta=0.48$. That A_r, and therefore $f_{21}(0)$, is relatively momentum-independent over the

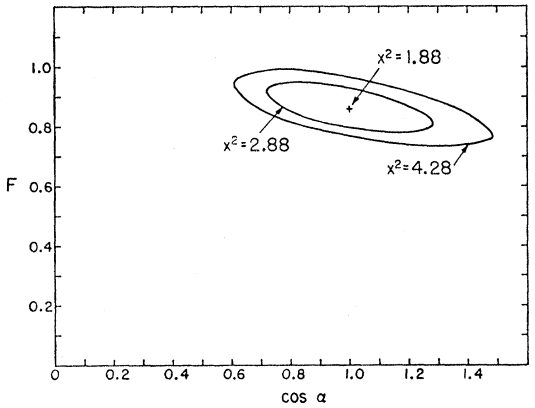

FIG. 14. Two-dimensional projection of χ^2 surface as a function of $\cos\alpha$ and the amplitude ratio $F=|A_R|/|\eta_{+-}|$. The minimum χ^2 occurs at $\cos\alpha=1.00$ and $F=0.86$. Also plotted are the one-standard-deviation and 90%-confidence contours. Integrating along the F axis gives a result for $\cos\alpha$ independent of the regeneration amplitude: $\cos\alpha=1.00\pm0.21$. This fit is independent of the K_1-K_2 mass difference.

range investigated in this experiment is again demonstrated in Fig. 15, which shows the momentum distribution of those events accepted from free decay and from the 0.40-g/cm³ regenerator.

The original demonstration of interference[3] was obtained by a comparison of the $\pi^+\pi^-$ rates from free decay, the 0.10 g/cm³ regenerator, and the rate from a solid slab of Be. To a first approximation the latter data determines $|f_{21}(0)|^2$, and providing the mass difference is known the contribution from the beryllium in the diffuse regenerator and thence $\cos\alpha$ may be calculated. To make the result independent of detection efficiency the solid regenerator data were taken at 4-in. intervals along the beam throughout the event region. These rates were averaged to calculate a mean event rate. This rate was corrected for regeneration in the $\frac{1}{8}$-in. anticoincidence counter set behind the slab and for the interference between the regenerated amplitude and the

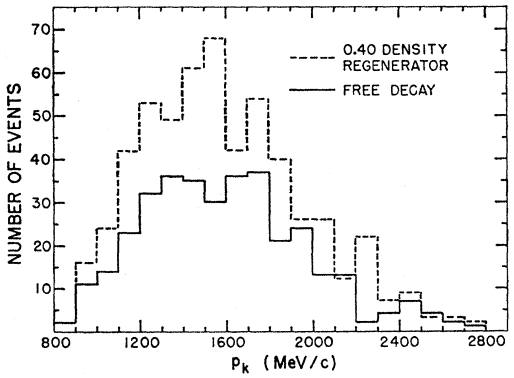

FIG. 15. Momentum distribution of detected $\pi^+\pi^-$ events from free K_2^0 decay in air (solid curve) and from the 0.4 regenerator (dashed curve). The distributions are very similar, indicating that the regeneration amplitude A_r has the same momentum dependence as η_{+-}, i.e., nearly constant.

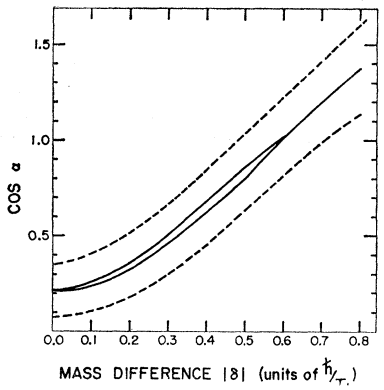

FIG. 16. Interference angle as function of K_1-K_2 mass difference δ, obtained by comparing $\pi^+\pi^-$ rates from free decay, 0.1 regenerator and regeneration from a single slab of Be. Because the latter data are corrected for interference, the curve is double valued in the physical region. The correction depends on the sign of the product $\alpha\delta$, and the upper branch corresponds to $\alpha\delta<0$. The abscissa should be multiplied by 0.71.

free-decay amplitude behind the slab. Because the latter correction depends on $\cos\alpha$, the solution was obtained by iteration. The correction also depends on the sign of $\alpha\delta$. The resulting solution, shown in Fig. 16 as a function of mass difference δ, is double valued. At the current best value of $|\delta|=0.48\pm0.02$, we obtain

$$\cos\alpha=1.18\pm0.23.$$

This is consistent with the mass-difference–independent measurement but, we emphasize, it is not independent since some data are common. The solid Be data yield

$$|f_{21}(0)|=2.38\pm0.35\ \text{F}.$$

VI. INTERPRETATION OF RESULTS AND CONCLUSIONS

In the search for a possible energy dependence in the branching ratio $R=(K_2\to\pi^+\pi^-)/(K_2\to\text{all charged modes})$ this experiment explores the range from 0.8 to 2.8 GeV/c. If the energy dependence is expressed as $R=R_0\gamma^n$, where γ is the energy, we find, from this experiment alone,

$$R_0=1.90\times10^{-3}\quad\text{and}\quad n=0.03\pm0.33.$$

Combining these data with the branching ratios measured[14,21,22] at mean momenta of 2.35, 4.5, and 10.7 GeV/c strengthens the conclusion that there is no energy dependence. The results from the combined data are

$$R_0=1.85\times10^{-3}\quad\text{and}\quad n=0.04\pm0.08.$$

If the $\pi^+\pi^-$ decay products are interpreted as being due to a new particle X rather than originating from the K_2^0, then one can interpret an energy dependence of the branching ratio in terms of a mean decay rate of the X particle relative to the K_2^0. One assumes the production spectrum of the X to be the same as the K_2^0. We find

$$\Gamma(X)/\Gamma(K_2^0)=1.02\pm0.60.$$

Again including the results of the experiments at other momenta one obtains

$$\Gamma(X)/\Gamma(K_2^0)=1.10\pm0.25.$$

The fact that interference is also observed requires the X particle to be produced coherently with the K_2^0 and to have the same mass to within about one part in 10^{15}. Clearly, the X particle is identical with the K_2^0.[23]

Assuming no energy dependence, we obtain, from all the data quoted, a branching ratio

$$R=(1.99\pm0.08)\times10^{-3}.$$

Taking the K_2^0 decay rate to be $(1.94\pm0.05)\times10^7$ sec^{-1},[24] the $K_1^0\to\pi^+\pi^-$ rate to be $(7.99\pm0.19)\times10^9$ sec^{-1}, and the ratio $(K_2^0\to\text{all charged modes})/(K_2^0\to\text{all modes})=0.76\pm0.03$, we obtain

$$|\eta_{+-}|=|\epsilon+\epsilon'|=(1.91\pm0.06)\times10^{-3}.$$

In the interference part of the experiment we determine $\cos\alpha=1.00\pm0.21$ independent of the mass difference and $\cos\alpha=1.18\pm0.23$ using solid Be data and a mass difference of 0.48. This demonstrates the highly constructive interference between A_r and η_{+-} in complete agreement with the conclusions presented in our preliminary report.[3]

From the mass-difference–independent result for $\cos\alpha$, we find the phase difference $\alpha=0\pm36°$. The phase of η_{+-} is therefore equal to the phase of A_r, within the errors. The phase of A_r is $\arg[if_{21}(0)/(i\delta+\frac{1}{2})]$ which, for a pure imaginary and negative $f_{21}(0)$, gives $+43°$. As indicated in Ref. 3, optical-model calculations[25] show $f_{21}(0)$ to be largely imaginary for values of the real parts of the K^0-$\bar{K}^0$ nucleon scattering amplitudes suggested by the data available.[26] If we consider only the imaginary parts of the K^0 and $\bar{K}^0$ scattering amplitudes as obtained, via the optical theorem and charge symmetry, from the highly precise $K^\pm$-nucleon total-cross-section data of Cool *et al.*,[27] we find from an optical

[21] X. DeBouard, D. Dekkers, B. Jordan, R. Mermod, T. R. Willitts, K. Winter, P. Scharff, L. Valentin, M. Vivargent, and M. Bott-Bodenhausen, Phys. Letters **15**, 58 (1965); *ibid.* (to be published).

[22] W. Galbraith, G. Manning, A. E. Taylor, B. D. Jones, J. Malos, A. Astberry, N. H. Lipman, and T. G. Walker, Phys. Rev. Letters **14**, 383 (1965).

[23] For one residual reservation see P. Kabir and R. Lewis, Phys. Rev. Letters **15**, 306 (1965); **15**, 711 (1965).

[24] T. Devlin, J. Solomon, P. Shepard, E. Beall, and G. Sayer, Phys. Rev. Letters **18**, 54 (1967).

[25] S. Fernbach, R. Serber, and T. Taylor, Phys. Rev. **75**, 1352 (1949).

[26] V. Cook, B. Cork, T. Hoang, D. Keefe, L. Kerth, F. Murphy, W. Wenzel, and T. Zipf, Phys. Rev. **129**, 2743 (1963); A. Fridman, O. Benary, A. Michalon, B. Schiby, R. Strub, and G. Zech, *ibid.* **145**, 1136 (1966); V. Cook, B. Cork, T. Hoang, D. Keefe, L. Kerth, W. Wenzel, and T. Zipf, *ibid.* **123**, 320 (1961).

[27] R. Cool, G. Giacomelli, T. Kycia, B. Leontic, K. K. Li, A. Lundby, and J. Teiger, (K^-): Phys. Rev. Letters **16**, 1228 (1966); (K^+): *ibid.* **17**, 102 (1966).

model that $\mathrm{Im}f_{21}(0)=2.52$ F. We use a uniform model with a radius of 3.39 F as given by fits to pion-nucleon scattering.[20] The results are independent of shape for nuclei as small as Be.

Recently Cool *et al.* have measured the cross sections down to 21 mrad for K^+ and K^- on Be at the mean momentum of this experiment, 1.55 GeV/c. Extrapolations to zero angle give 160 ± 3 mb and 225 ± 4 mb for the K^+ and K^- total cross sections. The K^0 and $\bar{K}^0$ cross sections differ from these because (a) Be^9 is not charge symmetric and (b) there is interference between the real parts of the nuclear and the Coulomb potentials. The optical model is used as a guide to make the small correction for the lack of charge symmetry. We have estimated the interference effect on the basis of the Born approximation using a ratio of real-to-imaginary amplitudes of -0.3 for K^- and -0.5 for K^+. This leads to constructive interference for K^+ and destructive for K^-. Including effects (a) and (b) we obtain 155 ± 3 mb and 230 ± 4 mb for the total cross sections of K^0 and $\bar{K}^0$ on Be. From these cross sections we obtain $\mathrm{Im}f_{21}(0) = -(2.33\pm0.16)$ F where the errors are purely statistical. Because of the sensitivity to the assumptions made in correction (b) the result is scarcely definitive. However, the agreement with the optical model is good.

Combining the experimental results from the diffuse regenerator studies and the solid Be data we obtain (for $|\delta|=0.48$) $|f_{21}(0)|=2.56\pm0.21$ F. Comparing this result with the results above for $\mathrm{Im}f_{21}(0)$, we see that $f_{21}(0)$ is largely imaginary. Because we measure the cosine of the phase angle, we are insensitive to the presence of small real parts.

In retrospect the highly constructive interference observed in this experiment is not surprising. It has been shown by many authors that the phase of ϵ must be $\arg[1/(i\delta+\frac{1}{2})]=44°$ to within about 10°, if ϵ' is zero. If ϵ' is nonzero, as recent measurements indicate,[28] its phase is governed by the $J=0$ $\pi\pi$ phase shifts. Recent extrapolations from multipion production[29] give $\delta_0-\delta_2 = 53°\pm15°$. An analysis of K^+ decay[8] assuming $\Delta I=\frac{3}{2}$ yields $\delta_0-\delta_2=66°\pm13°$. To the extent that these deductions are valid, the phase of ϵ' is expected to be $\approx30°$ to within 180°. Therefore, independent of how the effect is distributed between ϵ and ϵ', the phase of $\eta_{+-}\approx30°$ $-45°$. As we have seen, a largely imaginary scattering amplitude leads to a phase of $A_r\approx45°$, thereby accounting for the effect. A summary of the other existing information on the phase of η_{+-} is given by Mischke *et al.*[15] In no case does the data decisively determine whether CP violation is predominantly in ϵ or ϵ'.

The branching ratio

$$\Gamma(K_2^0\to\mu^+\mu^-)/\Gamma(K_2^0\to\text{all charged modes}) \leq 3.5\times10^{-5} \quad (90\%\text{ confidence level})$$

may be interpreted[30] as a limit on the ratio of the neutral to the charged coupling constants. We find at the 90% confidence level

$$|g_{\mu\mu}/g_{\mu\nu}|^2\leq2.5\times10^{-6}.$$

Finally, we end this report on a philosophical note which has been emphasized to us by Sakurai and Wattenberg (private communication). It is that an antiphysicist doing this experiment in his antilaboratory would observe essentially destructive interference instead of the constructive interference observed here. In short, it is possible through this experiment to distinguish world from antiworld without reference to any outside system. This is most easily seen by observing that N_{+-} [Eq. (5)] changes sign in going from an initially pure K^0 state to an initially pure $\bar{K}^0$ state. However, with antimatter in the beam there is an additional change in the sign of the $R-S$ term of Eq. (5) if one assumes C invariance in the strong interactions. Because the K^0-nucleon amplitude then equals the $\bar{K}^0$-antinucleon scattering amplitude the regeneration in antimatter is described by $-f_{21}(0)$ resulting in the change in sign of A_r relative to η_{+-}.

ACKNOWLEDGMENTS

We wish to thank the engineers and operations crew of the AGS for their assistance and cooperation. Professor D. Bartlett, Professor D. Cassel, Professor J. Cronin, Dr. D. Hutchinson, and Dr. R. Turlay gave valuable assistance in early stages and K. Peterson, B. Bowman, and D. Perlman lent helping hands in taking and analyzing the data. We also thank Professor S. B. Treiman for many illuminating discussions. We are also indebted to our shop crew for their work in building the apparatus and to our scanning staff. The spectrometer magnet was loaned to us by the Princeton-Pennsylvania accelerator. This work made use of the Princeton computer center, supported in part by NSF Grant No. NSF-GP579.

[28] J. Cronin, P. Kunz, W. Risk, and P. Wheeler, Phys. Rev. Letters **18**, 25 (1967); J. M. Gaillard, F. Krenien, W. Galbraith, A. Hussri, M. Jane, N. Lipman, G. Manning, T. Ratcliffe, P. Day, A. Parham, A. Sherwood, B. Payne, H. Faissner, and H. Reither, *ibid.* **18**, 20 (1967).

[29] W. Walker, J. Carroll, A. Garfinkel, and B. Oh, Phys. Rev. Letters **18**, 630 (1967).

[30] T. D. Lee and C. N. Yang, Phys. Rev. **119**, 1410 (1960).